Nonequilibrium spin polarization of F centers in KBr and KI under saturated optical pumping with modulated circular polarization

Norio Akiyama

Department of Electronic Engineering, Okayama University of Science, 1-1 Ridai-cho, Okayama 700, Japan

Hiroshi Ohkura

Department of Applied Physics, Osaka City University, 3-3-138 Sugimoto, Sumiyoshi-ku, Osaka 558, Japan

It has been known that, under the saturated optical pumping of an F center in the presence of an applied magnetic field (H), the nonequilibrium spin polarization (NESP) increases in the relaxed excited state (RES) of the F center. The NESP is relevant to a spin-lattice relaxation time T_1^* in the spin system in the RES. Under conditions in which the circular polarization of the pumping light is modulated between right and left circular polarization with an angular frequency ω, we postulate that the NESP oscillates sinusoidally with ω and gives rise to the magnetic circular dichroism in the absorption, $\mathcal{S}_{MCD}(\omega)$, and the magnetic circular polarization in the emission, $\Delta_\eta(\omega)$, where η shows the polarization of the analyzer, either circular or linear. Theoretical forms of both quantities have been derived from the first-order approximation to successive solutions of rate equations. $\Delta_\eta(\omega)$ for KBr and KI have been measured at 2 K as a function of H below 40 kOe and as a function of pumping photon energy. Our present data for $\Delta_\eta(\omega)$ and $\mathcal{S}_{MCD}(\omega)$, observed by Baldacchini *et al.* [Phys. Rev. B **19**, 1283 (1979)], are both explained in the same theoretical framework by introducing a common empirical form of H dependence of $(T_1^*)^{-1}$, which is presented as proportional to H^α, where α is a negative constant. This implies that the spin-lattice relaxation is caused by the exchange effects between two F centers in the RES. We have optically detected the electron-spin resonance (ODESR) of F centers in the RES from the changes observed in $\Delta_\eta(\omega)$ by the resonant microwave at 50 GHz. The ODESR has been accounted for within the same theoretical framework.

I. INTRODUCTION

For almost the past two decades the spin dynamics of the optically excited (or pumped) F centers in alkali halides under the application of a static magnetic field H has been studied. The most remarkable magnetic effects observed in the optical-pumping cycle (OPC) are the magnetic circular dichroism (MCD) in the optical absorption[1-5] and the magnetic circular polarization (MCP) in the emission.[6-16] Both effects have been measured by pumping with F-band light with left- and right-circular polarization components (σ_+ and σ_-), or a linearly polarized light (π). Under the *steady-pumping condition,* where the polarization of pumping light is fixed at π or $\sigma_\pm$, the MCD and MCP observed have been well analyzed and interpreted.[1-11] However, under the *modulated-pumping condition,* when the circular polarization of pumping light is periodically alternated between σ_+ and σ_- with an angular frequency ω, the complete physical pictures of MCD and MCP observed have not yet been completely clarified. We denote both quantities as $\mathcal{S}_{MCD}(\omega)$ and $\Delta_\eta(\omega)$, where the subscript η refers to the characteristic polarization ($=\sigma_+, \sigma_-,$ or π) of the analyzer, which is arranged to select the polarization in the emission. In particular, the observed quantity defined by

$$\Delta_\pi(\omega) = \tfrac{1}{2}[\Delta_{\sigma_+}(\omega) + \Delta_{\sigma_-}(\omega)] \qquad (1)$$

shows a large nonlinear dependence on H. Baldacchini *et al.* called it an anomalous effect.[7] Actually, they explained it by proposing, intuitively, an analytical form [see Eq. (17) in Ref. 7]. Therein, they concluded that it is not a quantity of true fundamental interest. Alternatively, in a previous work[15] we tentatively showed a different way of analyzing $\Delta_\pi(\omega)$. In the present work we show details of our argument. Hereupon, on the basis of the same theoretical framework, we derive a theoretical form to analyze the experimental data of $\mathcal{S}_{MCD}(\omega)$, which had been observed by Baldacchini *et al.*[12] They have left the task of exploring their data taken at a lower magnetic field range (below 40 kOe) for a future analysis.

Now, for the purpose of giving consistent analytical forms to explain both $\mathcal{S}_{MCD}(\omega)$ and $\Delta_\eta(\omega)$, we examine the time factors spent while an electron completes the OPC in the F center. Immediately after the electron is excited optically from the ground state (GS) to the Franck-Condon state (FCS), it dissipates its excess energy nonradiatively from the FCS to the relaxed excited state (RES) within a fraction of a picosecond.[17] Then, it returns to the GS by emitting luminescence, and terminates the OPC. The radiative lifetime τ_r of the RES has been determined to be a few microseconds or less.[18] This lifetime would be the shortest time limit in the argument of the magneto-optical effects modulated with ω. In the presence of a field H, the thermalizations in the Kramers sublevels in the GS and RES are characterized by the

spin-lattice relaxation times T_1 and T_1^*, respectively. In a moderate magnetic field range, the relation $\tau_r < T_1^* < T_1$ holds.[3] In addition to these factors, a spin flipping occurs during the OPC because of the spin-orbit interaction in the optically excited states.[3-5,10,16] This spin-flipping process causes the change of the spin polarization in both the GS and RES.[3-5,10,16] A net spin-flipping rate was expressed by $\varepsilon_t U$, where ε_t is a total spin-memory loss parameter and U is a net pumping rate.[14,19] With reference to $\varepsilon_t U$ and T_1, the optical pumping conditions are divided into two cases: the *weak pumping* for $\varepsilon_t U T_1 < 1$ and the *saturated pumping* for $\varepsilon_t U T_1 > 1$.[3,12-14] In the former case, the spin system can be treated as if it was in thermal equilibrium. The experimental data obtained under this condition have been well analyzed.[3] However, in the latter case the spin system should be treated as if it was in a nonequilibrium state, in which case the spin polarization should be considered a dynamical quantity. We refer to this case as the nonequilibrium spin polarization (NESP). A major part of the present work is devoted to determining how the NESP contributes to the magneto-optical effects, particularly in the determination of $\Delta_\eta(\omega)$ and $\mathscr{S}_{MCD}(\omega)$.

Under a combined case of the *steady- and saturated-pumping* (SSP) conditions pumped with a *π-polarized light*, the NESP in the GS has insufficient time to build up before the NESP in the RES is raised. The theoretical forms of the NESP in the GS and RES under the SSP conditions were derived from a zeroth-order solution to the rate equations that govern the OPC. Both forms are approximately equivalent to each other, as will be shown in Eqs. (9) and (18), and depend on T_1^* but not on T_1. This fact clearly shows that the as-described NESP in the RES could solely exert an influence on the magneto-optical effects in the OPC. On the other hand, the form of spin polarization in the RES derived under the SSP conditions pumped with σ_+- or σ_--polarization light is different from that in the GS, due to a predominantly large contribution from the paramagnetic term included.[7-10]

As a next step, let us discuss the magneto-optical effects observed in another combined condition, the *modulated- and saturated-pumping* (MSP) condition. In this case, the zeroth-order solutions of NESP to the rate equations for the GS and RES have already been derived in Ref. 14: this will be shown in Eqs. (17). Both forms are composed of a sum of ωt-independent and ωt-dependent terms. We denote the approximate form of the former term as P_{ms}, as will be shown in Eq. (18). The latter term is observable by means of lock-in detection operated at ω. However, we found that the form of $\Delta_\pi(\omega)$ in Eq. (1) derived in the zeroth-order approximation cannot account for the anomalous effect observed. We suggest that promotion to a higher-order approximation would give a proper solution to the difficulty. After a calculation in a specific condition $T_1^{-1} < \varepsilon_t U < \omega < \tau_r^{-1}$, we will show that the first-order approximation gives rise to partly a new term of the NESP, which has an amplitude $P_s P_{ms}$ oscillating with ω. Here, P_s is a dichroic differential absorption that will be defined in Eq. (3).[3,19]

This means that, as a result of the first-order approximation, the time-independent P_{ms} could oscillate. Finally, we confirm that P_{ms} will contribute essentially to the anomalous effect in Eq. (1).

Based on this scheme, we also derived an analytical form of $\mathscr{S}_{MCD}(\omega)$ in MSP conditions: this form is different from that derived in Refs. 1-5. It is worth noticing that both quantities $\Delta_\eta(\omega)$ and $\mathscr{S}_{MCD}(\omega)$ include a common parameter of T_1^*. Thus, from the curve-fitting analysis of the H dependence of both $\mathscr{S}_{MCD}(\omega)$ and $\Delta_\eta(\omega)$ using the above-derived theoretical forms, we may empirically determine the H dependence of T_1^*, $T_1^*(H)$. In other words, with a common form of $T_1^*(H)$, the $\mathscr{S}_{MCD}(\omega)$ and $\Delta_\eta(\omega)$ observed under the MSP conditions are explained consistently in the same theoretical framework.

The present paper consists of the following three sections. In Sec. II, we summarize several difficult problems and unresolved data arising from the previous studies of $\mathscr{S}_{MCD}(\omega)$ and $\Delta_\eta(\omega)$ observed under the MSP conditions. To resolve these difficulties, we formulate a series of rate equations that is improved particularly in that it includes an imbalance parameter ε_I of the σ_+ and σ_- polarization of pumping light. Section III is devoted to deriving the theoretical expressions of $\Delta_\eta(\omega)$ and $\mathscr{S}_{MCD}(\omega)$ by using the first-order approximated solution to the rate equations in Sec. II. In Secs. IV A and IV B, we analyze our experimental data on the H dependence of $\Delta_\pi(\omega)$ observed in KI and KBr at a fixed photon energy, E_{ph}, as well as the E_{ph} dependence of $\Delta_\eta(\omega)$ at a fixed H, using the theoretical forms derived in Sec. III. The same curve-fitting analysis of $\mathscr{S}_{MCD}(\omega)$ observed in Ref. 12 has been carried out. As a result, a consistent explanation of both quantities is achieved by introducing a common and empirical parameter of the $T_1^*(H)$ in the H range below 40 kOe: $[T_1^*(H)]^{-1}$ decreases with increasing H. In Sec. IV C, through comparison with the dependence of T_1 in the GS observed for the densely colored KCl, we suggest that the $T_1^*(H)$ in the low-field range is caused by the exchange effect between the exchange pair of F centers in the RES. In Sec. IV D, we develop a new optical detection method of the electron-spin resonance (ESR) for the GS and RES at 2 K. We have observed them from the variation of $\Delta_\eta(\omega)$ induced by the resonant microwave of 50 GHz at $H \sim 20$ kOe. The ESR signals can be explained consistently within the present theoretical framework.

II. PROBLEMS ARISING FROM THE PREVIOUS INTERPRETATION OF MCD AND MCP UNDER THE MODULATED AND SATURATED PUMPING CONDITIONS

A. Spin systems in the optical-pumping cycle

We summarize fundamentally important quantities to describe the OPC of the F center under the application of H. the model proposed is schematically illustrated in Fig. 1. The Kramers sublevels in the GS and RES are specified by the spin-quantum numbers of m_s and M_k,
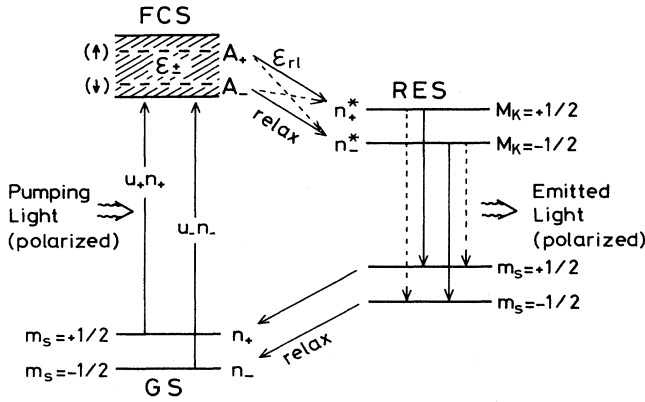
FIG. 1. Optical-pumping cycle of an F center in the presence of magnetic field. The spin-split Kramers doublets in the ground and relaxed excited states (GS and RES) are specified by the spin quantum numbers of m_s and M_k. The optical-pumping rates from the m_s levels in the GS to the Franck-Condon state (FCS) are denoted $u_\pm$ reflecting $m_s = \pm\frac{1}{2}$. The $\varepsilon_\pm$ and ε_{rl} are the spin-mixing parameters at the FCS and the nonradiative transition processes, respectively. $A_\pm \equiv (1-\varepsilon_\pm)u_\pm n_\pm + \varepsilon_\mp u_\mp n_\mp$.

which are $\pm\frac{1}{2}$.[3,8] The populations of sublevels are denoted $n_\pm$ and $n_\pm^*$: here, the subscripts show corresponding spin quantum numbers. The polarizations of the spin systems in the GS and RES, P and P^*, respectively, are defined in general by

$$P = n/N \qquad (2a)$$

and

$$P^* = n^*/N^* . \qquad (2b)$$

Here,

$$n = n_+ - n_- \quad \text{and} \quad N = n_+ + n_- \qquad (2c)$$

and

$$n^* = n_+^* - n_-^* \quad \text{and} \quad N^* = n_+^* + n_-^* . \qquad (2d)$$

When the spin systems are thermalized at a certain temperature T, both P and P^* represent the equilibrium values, which are $-\tanh(g\mu_B H/2kT)$ and $-\tanh(g^*\mu_B H/2kT)$, respectively, where g and g^* are the g factors in the GS and RES, μ_B is the Bohr magneton, and k is the Boltzmann constant. They are denoted $\langle P \rangle$ and $\langle P^* \rangle$, respectively. However, as was described in Sec. I, the spin systems are not always thermalized. In this case, the NESP should be determined from the solution of rate equations, as will be given in Sec. III A.

In the optical-absorption process, it is well established that the spin-orbit interaction in the FCS could give rise to the difference in the optical-pumping rates, $u_\pm$,[20] as well as the difference in the spin-memory loss parameters, $\varepsilon_\pm$. Both depend on the signatures $\pm$ of quantum number in the initial Kramers sublevels in the GS.[3-5,10,19]

For convenience, Mollenauer and Pan[3] introduced a dichroic differential absorption P_s, defined by

$$P_s = (u_- - u_+)/U , \qquad (3)$$

where U is the total pumping rate given by a sum of u_+ and u_-. They had measured P_s for KCl, KBr, and KI as a function of E_{ph}.[3] Instead of $\varepsilon_\pm$, Winnacker et al. introduced an anisotropic spin-mixing parameter and an isotropic one, $\delta\varepsilon$ and ε_0, defined as $\delta\varepsilon = \varepsilon_- - \varepsilon_+$ and $\varepsilon_0 = (\varepsilon_- + \varepsilon_+)/2$, respectively.[4,5] In Ref. 19 we have calculated both parameters as a function of E_{ph} by extending the Mauser et al. method.[4] The total spin-memory loss parameter in the OPC is given by $\varepsilon_t = \frac{1}{2}[1 - (1-2\varepsilon_0)(1-2\varepsilon_{rl})]$,[14,19] where ε_{rl} is a parameter which expresses a spin-memory loss occurring in the nonradiative process from the FCS to the RES.[9,14,19] Thus, the net spin-flipping rate in one OPC can be represented by $\varepsilon_t U$, as was discussed in Sec. I.

B. MCD of absorption

Mollenauer and Pan[3] have derived the form of MCD in the optical absorption under the modulated pumping condition. It is given by

$$\mathcal{S}_{MCD}(\omega) \equiv (I_+ - I_-)/(I_+ + I_-) = H/H_d + P_s P , \qquad (4)$$

where I_+ and I_- are the intensities of transmitted light with σ_+ and σ_- polarization, respectively, through a crystal, $1/H_d$ is the diamagnetic coefficient,[3,20,21] and P is the NESP in the GS defined in Eq. (2a).

Mollenauer and Pan[3] and Baldacchini et al.[12] derived an expression of P, when pumped with a light of π polarization, under the simplified condition that $U \ll \tau_r^{-1}$. It is given by

$$P = \{(T_p/T_1)\langle P \rangle + [L/(1+L)]\langle P^* \rangle\}/(1 + T_p/T_1) , \qquad (5)$$

with

$$T_p^{-1} = \varepsilon_t U(1+L)/(1+2\varepsilon_t L) \qquad (6)$$

and

$$L = \tau_r/(2\varepsilon_t T_1^*) . \qquad (7)$$

In Ref. 12, ε_t was replaced by ε.

In the extreme case when $L \ll 1$, Eq. (6) is reduced to $T_p^{-1} = \varepsilon_t U$. Equation (5) is simplified as follows:

$$P_{weak} = \langle P \rangle/(1 + \varepsilon_t UT_1) . \qquad (8)$$

P_{weak} could be reduced to $\langle P \rangle$ when $\varepsilon_t UT_1 \ll 1$ under a very-weak-pumping condition. In this case, the second term of $\mathcal{S}_{MCD}(\omega)$ in Eq. (4) is determined by $P_{weak} \simeq \langle P \rangle$,[20] because a majority of the F electrons are thermalized in the GS.[12]

In another extreme case of the saturated-pumping condition with π-polarized light, Eq. (5) is reduced to

$$P_{sat} = [L/(1+L)]\langle P^* \rangle , \qquad (9)$$

because T_p is approximately reduced to zero. According

to Ref. 12, an expression for the spin polarization in the RES, P_{sat}^*, which was derived under the SSP conditions pumped with π-polarized light, was found to coincide with Eq. (9). In the present work, as will be shown in Eq. (18), we show that the same relation holds approximately even under *the MSP conditions within a specific ω range of $\varepsilon_t U < \omega < \tau_r^{-1}$.*

Baldacchini et al.[12] measured $\mathscr{S}_{MCD}(\omega)$ for *F* center in KI and KBr under the MSP conditions and analyzed it by using Eqs. (4) and (9). From the analysis, they have determined the following empirical form of $T_1^*(H)$ in the range of magnetic field between 40 and 80 kOe:[22]

$$[T_1^*(H)]^{-1} = (A^*H^3 + B^*H^5)\coth(g^*\mu_B H/2kT) , \quad (10)$$

where A^* and B^* are fitting parameters: these are listed in Table I. Later, they confirmed that the H dependence of the diamagnetic component of the MCP observed under the SSP conditions, $\Delta_d(0)$ could be also analyzed by using Eq. (10) in the H range above 40 kOe.[11,12] However, it is unfortunate that they did not analyze the H dependence of both $\mathscr{S}_{MCD}(\omega)$ and $\Delta_d(0)$ below about 40 kOe. This will be done in Sec. IV B.

C. MCP of emission

The MCP of the *F* center was first observed in KF by Fontana and Fitchen in 1969.[6] The preliminary analysis of the MCP was done by Mollenauer and Pan in 1972.[3] Thereafter, the study was succeeded by Baldacchini, Grassano, and Tanga[7] in Italy. Independent of these schools, we carried out studies on MCP since 1974 at Osaka in Japan.[8-10]

Baldacchini et al. proposed intuitively that the form of the expression of $\Delta_\pi(\omega)$ in Eq. (1) is similar to that of $\mathscr{S}_{MCD}(\omega)$ in Eq. (4), and performed their analysis using Eq. (8) for *P*. As a result, they concluded that the $\Delta_\pi(\omega)$ is not a quantity of fundamental interest,[7] because it does not include any important quantities. We consider this adoption of P_{weak} in Eq. (8) unreasonable, because the pumping condition described in Ref. 7 would correspond to a saturated-pumping condition. We suspect that, instead of Eq. (8), they should have adopted P_{sat} in Eq. (9) for *P* in Eq. (4).

In Ref. 7, $\Delta_\pi(\omega)$ was observed when pumped with a single laser line of either a He-Ne or Ar$^+$-ion laser. On the other hand, we have measured $\Delta_\pi(\omega)$ as a function of H by pumping the *F* center with various laser lines from a dye laser pumped with an Ar$^+$-ion laser. The results are shown in Figs. 2 and 3 for KBr and KI, respectively. They show that the H dependence of $\Delta_\pi(\omega)$ is quite relevant to the pumping wavelengths. Moreover, the inversion of the sign is observed for the first time. These characteristics cannot be accounted for simply by adopting the idea mentioned in the preceding paragraph.[7] One of the main purposes of this work is to account for these observations using a rational analytical form of $\Delta_\pi(\omega)$, as will be derived in Eq. (28).

D. Improved rate equations of *F* center in OPC

Solutions of the rate equations of the OPC have been proposed by many authors[3-5,7-15] in an effort to explain the dynamical magneto-optical effects of the *F* center. The zeroth-order approximation was quite sufficient to perform the analysis of the experimental data obtained under the SSP conditions. However, the form of the solutions in the zeroth-order approximation could not account for the anomalous effect observed under the MSP conditions. To obtain suitable analytical forms, we propose a way to promote the zeroth-order approximation to a first-order approximation. This promotion is physically equivalent to include properly the saturated-pumping condition in which N and N^* in Eqs. (2c) and (2d) could *depend on time as well as on ω*, while the total number of N_t is kept constant. It is written as

$$N_t = N(\omega,t) + N^*(\omega,t) . \quad (11)$$

Notice that in the zeroth-order approximation both N and N^* are assumed to be independent of time and ω.

Finally, we should mention that we are occasionally faced with an unavoidable difficulty, which is caused by our experimental setup. There is an imbalance of the σ_+ and σ_- components of the incident pumping light, whose intensities are denoted I_+^i and I_-^i, respectively. The imbalance parameter could be represented by an imbalance parameter ε_I, which is defined by

$$\varepsilon_I = (I_+^i - I_-^i)/(I_+^i + I_-^i) . \quad (12)$$

TABLE I. Fitting parameters A^*, B^*, C^*, and α to Eq. (31) are obtained at 2 K. g^* values are from Ref. 31. Fitting parameters A^* and B^* to Eq. (10) determined by Baldacchini et al. at 1.85 K are also listed from Ref. 12.

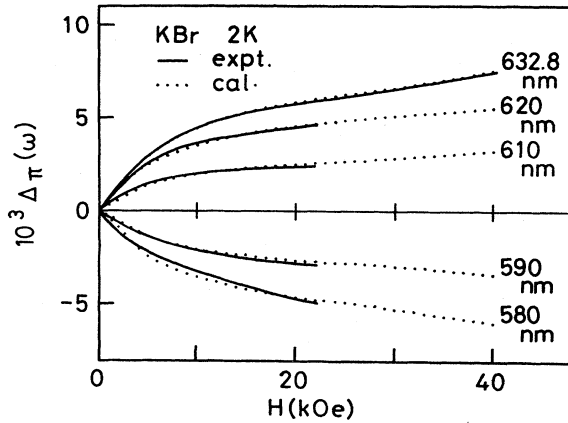| Crystals	T (K)	A^* (10^{-11} Oe^{-3}s^{-1})	B^* (10^{-21} Oe^{-5}s^{-1})	C^* (10^7 Oe$^{-\alpha}$s^{-1})	α	g^*
KBr	2	1.5	2.6	0.50	−0.613	1.873
	1.85	1.2	1.0	a	a	1.873
KI	2	8.5	15.5	1.13	−0.738	1.686
	1.85	5.7	6.0	a	a	1.686

aUndetermined.

FIG. 2. The magnetic field dependence of $\Delta_\pi(\omega)$ for the F center in KBr is plotted when the pumping photon wavelengths are varied at 2 K. Solid lines are experimental data, and dotted lines are the theoretical plot of Eq. (28) using $T_1^*(H)$ in Eq. (31). Fitting parameters are listed in Table I.

Taking into account ε_I, the quantities P_s and $\delta\varepsilon$ are modified in the following way:

$$P_s \rightarrow \varepsilon_I P_s + (1-\varepsilon_I)P_s \cos(\omega t) , \qquad (13a)$$

and

$$\delta\varepsilon \rightarrow \varepsilon_I \delta\varepsilon + (1-\varepsilon_I)\delta\varepsilon \cos(\omega t) . \qquad (13b)$$
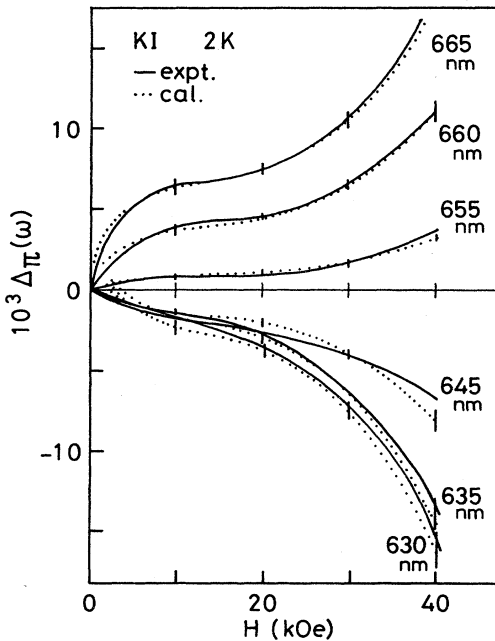

FIG. 3. The magnetic field dependence of $\Delta_\pi(\omega)$ for the F center in KI is plotted when the pumping photon wavelengths are varied at 2 K. Solid lines are experimental data, and dotted lines are the theoretical plot of Eq. (28) using $T_1^*(H)$ in Eq. (31). Fitting parameters are listed in Table I.

Thus, regarding Fig. 1 and including Eqs. (13), the rate equations of N, N^*, n, and n^* in Eqs. (2c) and (2d) are written as follows:

$$dN/dt = -(U/2)N + (1/\tau_r)N^*$$
$$+ (U/2)[\varepsilon_I P_s + (1-\varepsilon_I)P_s\cos(\omega t)]n , \qquad (14a)$$

$$dN^*/dt = -dN/dt , \qquad (14b)$$

$$dn/dt = \{(U/2)[\varepsilon_I P_s + (1-\varepsilon_I)P_s\cos(\omega t)] + \langle P \rangle/T_1\}N$$
$$- (U/2 + 1/T_1)n + (1/\tau_r)n^* , \qquad (14c)$$

and

$$dn^*/dt = (U/2)(1-2\varepsilon_{rI})[\varepsilon_I\kappa + (1-\varepsilon_I)\kappa\cos(\omega t)]N$$
$$+ (\langle P^* \rangle/T_1^*)N^* + (U/2)(1-2\varepsilon_t)n$$
$$- (1/\tau_r + 1/T_1^*)n^* , \qquad (14d)$$

with $\kappa = \delta\varepsilon - (1-2\varepsilon_0)P_s$. Hereupon, we assume that the term containing $(\delta\varepsilon)P_s$ in Eq. (14d) is negligibly small, since the amounts of both $\delta\varepsilon$ and P_s are less than unity.[19] We call Eqs. (14) the improved rate equations, due primarily to the inclusion of ε_I terms.[3-5] The value of ε_I can be determined from the computer-aided best-fit analysis of experimental data so that, by not including ε_I terms, we may obtain genuine magneto-optical effects. The procedure will be shown in Sec. IV A.

It is worth mentioning that Baldacchini et al. have pointed out that, in their measurement of $\Delta_d(0)$,[11] the effect of the imbalance of the pumping light is caused by the induced birefringence of a cooled window of the optical cryostat. They intended to prevent the imbalance effect by adjusting a birefringent plate manually in their measurement of $\mathscr{S}_{\text{MCD}}(\omega)$.[12]

III. THEORY

A. First-order approximated solutions of rate equations

Taking into account Eq. (11), the NESP in Eqs. (2a) and (2b) are expressed as

$$P(\omega,t) \equiv n(\omega,t)/N(\omega,t) ,$$
$$P^*(\omega,t) \equiv n^*(\omega,t)/N^*(\omega,t) . \qquad (15)$$

Let us calculate Eqs. (15) by solving Eqs. (14). In the zeroth-order approximation, N and N^*, which are denoted N_0 and N_0^*, can be easily derived from Eqs. (11) and (14a) by assuming that n and n^* are negligibly small in comparison with N and N^*. They are represented as follows:

$$N_0 = (1 + \tau_r U/2)^{-1}N_t ,$$
$$N_0^* = [1 + 2/(\tau_r U)]^{-1}N_t . \qquad (16)$$

Equations (16) are also equal to the solutions of Eqs. (14) in the steady-state condition. The zeroth-order approximated forms of n and n^*, which are denoted n_0 and n_0^*, are derived by inserting Eqs. (16) into Eqs. (14c) and (14d). This had been already done in Refs. 14 and 15. The zeroth-order approximated forms of Eqs. (15), which

are denoted $P_0(\omega,t)$ and $P_0^*(\omega,t)$, are rewritten as follows;

$$P_0(\omega,t)=P_m+|P_m(\omega)|\cos(\omega t +\phi) , \qquad (17a)$$

$$P_0^*(\omega,t)=P_m^*+|P_m^*(\omega)|\cos(\omega t +\gamma) , \qquad (17b)$$

where ϕ and γ are the phase factors, and the exact forms of P_m, P_m^*, $|P_m(\omega)|$, and $|P_m^*(\omega)|$ are summarized in the Appendix. The approximate forms of the last two quantities were already derived in Ref. 14 under the conditions that $\varepsilon_t U < \omega < \tau_r^{-1}$ and T_1 and T_1^* are infinite. They are expressed as $(\tau_r U/2)|P_s|$ and $(1-2\varepsilon_{rl})|\kappa|$, respectively. A comparison of these forms with those derived by other authors is given in the Appendix.

As will be shown in the Appendix, within a specific ω range defined as $T_1^{-1} < \varepsilon_t U < \omega < \tau_r^{-1}$ and $T_1 \gg T_1^*$, P_m and P_m^* are approximated into the same forms derived under the MSP conditions. From now on, we derive theoretical forms solely in this specific ω range unless otherwise stated. Hereafter, we denote both quantities as P_{ms} and P_{ms}^*. They are of equal amounts and are expressed as

$$P_{ms}=P_{ms}^*=[L/(1+L)]\langle P^* \rangle . \qquad (18)$$

Here, the factor $L/(1+L)$ in Eq. (18) reveals the efficiency of thermal spin flipping at the RES. Notice that Eq. (18) is of exactly the same form as Eq. (9), which was derived in the saturated-pumping condition. Equation (18) implies that, because of a much larger value of T_1 compared with those of $(\varepsilon_t U)^{-1}$ and T_1^*, the spin system cannot be thermalized in the GS before it attains the NESP in the RES while pumping with U. Once the NESP in the RES was established, it could apparently circulate in the OPC with pumping rate U. As a result, we propose that, in the case of modulation pumping, the NESP could give rise to the $\mathcal{S}_{\mathrm{MCD}}(\omega,t)$ and $\Delta_\eta(\omega,t)$, which are sinusoidally oscillating with ω. We suggest that these theoretical forms, which are valid in the MSP conditions, can be derived by promoting the successive approximation by one rank.

With a usual mathematical procedure, the first-order approximated solution of N, which is denoted N_1, is derived by substituting $n_0(\omega,t)=N_0 P_0(\omega,t)$ into n in Eq. (14a). Since the MCP can be measured by means of a lock-in detector operated at ω, the oscillating term of 2ω and transient attenuation terms in the solution of rate equations are unnecessary to represent here. After a tedious calculation omitting unimportant terms,[23]

$$N_1(\omega,t)\simeq N_0\{ 1+(\tau_r U/2)|P_s[P_{ms}+\varepsilon_I P(\omega=0, t=0)]|$$

$$\times\cos(\omega t +\phi)\} , \qquad (19)$$

where

$$P(\omega=0, t=0)=(1-2\varepsilon_{rl})\delta\varepsilon/[2\varepsilon_t(1+L)]+P_s$$

$$=P^*(\omega=0, t=0)/(1+L)+P_s . \qquad (20)$$

Here, $P(\omega=0, t=0)$ and $P^*(\omega=0, t=0)$ are the spin polarization in the GS and RES, respectively, under the SSP conditions. In a previous work,[10] we directly derived

Eq. (20). Similarly, from Eq. (19), using the relation of Eq. (11) and $N_0^* =(\tau_r U/2)N_0$ that was derived from Eqs. (16), $N_1^*(\omega,t)$ is calculated as follows:

$$N_1^*(\omega,t)\simeq N_0^* \{1- |P_s[P_{ms}+\varepsilon_I P(\omega=0, t=0)]|$$

$$\times\cos(\omega t +\phi)\} . \qquad (21)$$

Two sorts of second terms in Eqs. (19) and (21) are newly derived as a result of the first-order approximation under the MSP conditions. They show that the N_1 and N_1^* have terms which could vary sinusoidally with angular frequency ω. This fact really reveals the physical meaning of time-dependent $N(\omega,t)$ and $N^*(\omega,t)$ in Eq. (11). It is clear that their sum exactly satisfies Eq. (11).

Thereafter, we evaluate the contribution from the higher-order solutions of Eqs. (14). The value of the first-order approximated forms of n and n^* calculated by using N_1 and N_1^* are about $10^{-3}n_0$ and $10^{-3}n_0^*$. Next, using $n \sim n_0+n_1$ and $n^* \sim n_0^* +n_1^*$, the orders of the second-order approximated terms of N and N^* are estimated to be about 10^{-5} times smaller than N_1 and N_1^*. Therefore, we may neglect these contributions in the explanation of the observed $\mathcal{S}_{\mathrm{MCD}}(\omega)$ and $\Delta_\eta(\omega)$.

Finally, let us study the phase factors γ and ϕ in Eqs. (17). They depend on E_{ph}, and are expressed by[14]

$$\gamma \simeq 180°\zeta^* +\tan^{-1}(-\tau_r\omega) \qquad (22)$$

and

$$\phi \simeq 180°\zeta' +\tan^{-1}(-\tau_r\omega) . \qquad (23)$$

Here, ζ^* and ζ' depend on E_{ph}. Namely, when E_{ph} exceeds the peak energy (E_0) of the F band, ζ^* becomes 1. However, when $E_{\mathrm{ph}} < E_0$, ζ^* becomes 0. A similar but inverse relation holds for ζ', such as being 0 when $E_{\mathrm{ph}} > E_0$, and 1 when $E_{\mathrm{ph}} < E_0$. Thus, we find that the shift in the phase angle between γ and ϕ is approximately 180°. This approximate phase relation can be used in the proceeding subsections to explain the inversion of sign of $\Delta_\pi(\omega,t)$ observed in Figs. 2 and 3.

B. Calculations of $\Delta_\eta(\omega)$ and $\mathcal{S}_{\mathrm{MCD}}(\omega)$

Let us derive a theoretical expression for $\Delta_\eta(\omega)$. The observed value of $\Delta_\eta(\omega)$ is related actually to the intensity of F emission, $\mathbb{I}_\eta$, after passing through an analyzer fixed at η polarization.

Now, the emission intensity with σ_+ polarization emitted from the Kramers sublevels of $M_k = +\frac{1}{2}$ and $-\frac{1}{2}$ in the RES are written as $I_{\sigma_+}^H(+)$ and $I_{\sigma_+}^H(-)$, respectively (see Fig. 1). By setting the corresponding populations in each level as $n_\pm^*(\omega,t)$, a total intensity $\mathbb{I}_{\sigma_+}$ is given by

$$\mathbb{I}_{\sigma_+}=I_{\sigma_+}^H(+)n_+^*(\omega,t)+I_{\sigma_+}^H(-)n_-^*(\omega,t)$$

$$=\frac{1}{2}\{ [I_{\sigma_+}^H(+)+I_{\sigma_+}^H(-)]N^*(\omega,t)$$

$$+[I_{\sigma_+}^H(+)-I_{\sigma_+}^H(-)]n^*(\omega,t)\} . \qquad (24)$$

Substituting Eqs. (15), (17), and (21) into Eq. (24), and using the experimental condition that $[I_{\sigma_+}^H(+) -I_{\sigma_+}^H(-)]P_{ms}^* \ll [I_{\sigma_+}^H(+)+I_{\sigma_+}^H(-)]$, we find

$$\mathbf{I}_{\sigma_+} = \frac{1}{2} N_0^* [I_{\sigma_+}^H(+) + I_{\sigma_+}^H(-)]$$

$$\times \left[1 + \frac{I_{\sigma_+}^H(+) - I_{\sigma_+}^H(-)}{I_{\sigma_+}^H(+) + I_{\sigma_+}^H(-)} |P_{ms}^*(\omega)|\cos(\omega t + \gamma) - |P_s[P_{ms} + \varepsilon_I P(\omega=0, t=0)]|\cos(\omega t + \phi) \right] . \tag{25}$$

The third term in Eq. (25) is a specific term obtained in the first-order approximation, because two other terms in Eq. (25) are the same as those derived in the zeroth-order approximation.[14] On the other hand, $\Delta_{\sigma_+}(\omega,t)$ has been experimentally determined as $(1/a_1)(V_{ac}/V_{dc})$, where a_1 is the instrumental constant of a stress optical modulator, and V_{dc} and V_{ac} are the dc and ac components, respectively, of the emission intensity passed through the σ_+ polarizer.[7,14] The first term in Eq. (25) corresponds to V_{dc}, and the other two terms correspond to V_{ac}, which oscillates with ω. Thus, $\Delta_{\sigma_+}(\omega,t)$ is represented as

$$\Delta_{\sigma_+}(\omega,t) \simeq \frac{I_{\sigma_+}^H(+) - I_{\sigma_+}^H(-)}{I_{\sigma_+}^H(+) + I_{\sigma_+}^H(-)} |P_{ms}^*(\omega)|\cos(\omega t + \gamma)$$

$$- |P_s[P_{ms} + \varepsilon_I P(\omega=0, t=0)]|$$

$$\times \cos(\omega t + \phi) . \tag{26}$$

In Ref. 14, we showed that the ratio $[I_{\sigma_+}^H(+) - I_{\sigma_+}^H(-)]/[I_{\sigma_+}^H(+) + I_{\sigma_+}^H(-)]$ of the first term in Eq. (26) was reduced to $F_p + GH$, where F_p and G are proportionality constants defined therein. Furthermore, we estimated that the value of GH in the present H range is negligibly small compared to that of F_p, so that the GH term can be neglected.[23]

In the same manner used to derive Eq. (26), we have also calculated the forms of $\Delta_{\sigma_-}(\omega,t)$ and $\Delta_{\pi}(\omega,t)$. The calculation is not given here because of limited space.[23] With the phase relations obtained in Eqs. (22) and (23), these formulas are generalized as follows:

$$\Delta_\eta(\omega,t) = \xi\Delta_p(\omega,t) + \Delta_\pi(\omega,t)$$

$$= \{ \xi F_p |P_{ms}^*(\omega)| + |P_s[P_{ms} + \varepsilon_I P(\omega=0, t=0)]| \}$$

$$\times \cos(\omega t + \gamma) . \tag{27}$$

Here, $\xi = \pm 1$ correspond to polarizations $\eta = \sigma_\pm$, and $\xi = 0$ to $\eta = \pi$. We should emphasize that the second term in Eq. (27) is a new term derived from the present first-order approximation. This shows that the NESP, which is raised dynamically in the RES even under the SSP conditions, could cause the η component of the MCP to oscillate sinusoidally with ω in the MSP conditions, while the NESP can circulate in the OPC with frequency $\varepsilon_t U$. Furthermore, we point out that the amplitude of the second term is larger than that of the first term, reflecting the fact that $|P_s| \gg |F_p|$, even if $|P_{ms}| < |P_{ms}^*(\omega)|$. For example, the orders of magnitude of these quantities were estimated as $|P_{ms}| \simeq 7.5 \times 10^{-2}$, $|P_{ms}^*(\omega=2\pi \times 20.8 \text{ kHz})| \simeq 0.2$,[14] $|P_s| \simeq 8.5 \times 10^{-2}$,[3] and $|F_p| \simeq 4.5 \times 10^{-3}$,[14] at 632.8 nm and 20 kOe in KBr. This evidence supports the idea that our theoretical form

is suitable to account for $\Delta_\eta(\omega)$. The form is also advantageous in the estimation of the optical detection of ESR, which will be described in Sec. IV D. Finally, we should mention that γ in Eq. (27) is the same phase angle defined as $-\beta$ in Eq. (1) in Ref. 15. Because γ depends on E_{ph},[14] it causes the change of the sign of $\Delta_\eta(\omega,t)$ when E_{ph} varies. This change is experimentally observed, as shown in Figs. 2 and 3.

When we measured $\Delta_\eta(\omega,t)$ using a lock-in amplifier operated at ω, the amplitude given in Eq. (27) could be detected. We denote them as $\Delta_\eta(\omega)$. Referring to Eq. (27), the anomalous effect of $\Delta_\pi(\omega)$ defined in Eq. (1) is naturally deduced to be

$$\Delta_\pi(\omega) = P_s[P_{ms} + \varepsilon_I P(\omega=0, t=0)] . \tag{28}$$

Notice that the imbalance parameter ε_I in Eq. (12) plays an important role in evaluating $\Delta_\pi(\omega)$, because the values of $\varepsilon_I P(\omega=0, t=0)$ for a certain crystal show the same amount as P_{ms}. In Ref. 14, we defined the paramagnetic component $\Delta_p(\omega)$ by $\frac{1}{2}[\Delta_{\sigma_+}(\omega) - \Delta_{\sigma_-}(\omega)]$. The expression for $\Delta_p(\omega)$ calculated from Eqs. (27) and (28) agrees completely with that derived in Ref. 14, because the first-order forms are canceled automatically. This verifies the validity of the previous works on $\Delta_p(\omega)$ by Baldacchini et al.[7,13] and by us.[14,16,19]

Finally, on the basis of the same theoretical scheme, we derived an expression for $\mathscr{S}_{MCD}(\omega)$ in Eq. (4) for the absorption. Using the ε_I term in Eq. (12) and Eqs. (19)–(22), $\mathscr{S}_{MCD}(\omega)$ is derived as follows, since $P_m(\omega) \simeq 0$ in Eqs. (17):

$$\mathscr{S}_{MCD}(\omega) = x\alpha_0[-P_s P_{ms} + (\tau_r U/2)\Delta_\pi(\omega)] + \zeta H/H_d , \tag{29}$$

where x is the thickness of the crystal, α_0 is the absorption coefficient $(x\alpha_0 \ll 1)$ at $\omega=0$, and ζ takes the same sign as P_s, which depends on E_{ph}. It should be worth noticing that Eq. (29) shows the same form as Eq. (4), excluding the second term in Eq. (29), in which ε_I is included. However, as mentioned in Sec. II B, the quantity P in Eq. (4) should be definitely represented by P_{ms}.

In conclusion, we emphasize that both forms of $\mathscr{S}_{MCD}(\omega)$ in Eq. (29) and $\Delta_\pi(\omega)$ in Eq. (28) are correlated to each other by a common factor P_{ms} in Eq. (18), which is a function of $T_1^*(H)$.

IV. EXPERIMENTAL RESULTS AND DISCUSSION

A. Anomalous effect

We have measured the anomalous effect of the F centers in KBr and KI, $\Delta_\pi(\omega)$, at 2 K as a function of H up to about 40 kOe with a fixed photon energy E_{ph}.[15,16]

The circular polarization of the laser light from a tunable dye laser (Spectra-Physics 375) pumped with an Ar^+-ion laser (Spectra-Physics 165-09) was periodically alternated between σ_+ and σ_- with an angular frequency of ω ($\sim 2\pi \times 20$ kHz) by means of a stress optical modulator. Here, the $\Delta_\pi(\omega)$ is obtained as the emission intensity detected after passing through an analyzer with linear polarization. The experimental data of $\Delta_\pi(\omega)$ for KBr and KI are plotted in Figs. 2 and 3 with solid lines as a function of H, at a fixed wavelength or E_{ph} that can be varied. As shown in both figures, the observed H dependence of $\Delta_\pi(\omega)$ including its signature depends substantially on E_{ph}. It is found that the H dependence of $\Delta_\pi(\omega)$ at the pumping wavelength near a He-Ne laser line in Figs. 2 and 3 reproduces the result by Baldachini et al., except for the signature.[7]

Let us first determine the parameters ε_I and $T_1^*(H)$ empirically, and then analyze $\Delta_\pi(\omega)$. The $\Delta_\pi(\omega)$ observed in KBr and KI at a fixed magnetic field are also plotted in Figs. 4 and 5 as a function of E_{ph}. The solid lines are the best fit of Eq. (28) by choosing suitable values of ε_I and T_1^*. These values are tabulated in Table II in a case when H is fixed at 18 kOe for KBr and at 3 kOe for KI. The same sort of fitting procedure is carried out to determine the values of ε_I and T_1^* for several cases with varied H. With these values, the average value of ε_I, as well as the H dependence of $T_1^*(H)$, are determined below 40 kOe. Note that the term including ε_I gives a considerably large contribution in KI, particularly in the region of both tails of the F absorption band. However, its contribution for KBr is small over the whole F absorption band. The values thus obtained for $T_1^*(H)$ at 2 K
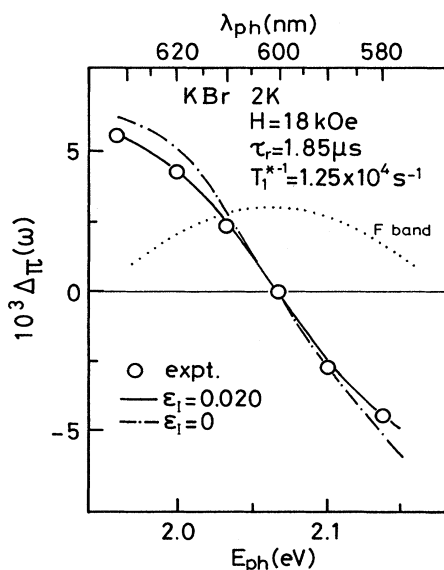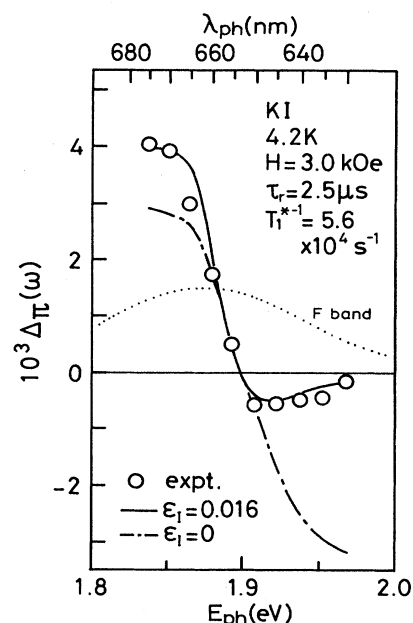

FIG. 5. $\Delta_\pi(\omega)$ for the F center in KI is plotted as a function of E_{ph} at $H = 3$ kOe and 4.2 K. Open circles are experimental points. Solid and dotted-dashed lines are theoretical plots of Eq. (28) with $\varepsilon_I = 0.016$ and 0, respectively. Dotted line is the F absorption band.

are plotted with open circles and open triangles for KBr and open diamonds for KI in Fig. 6 as a function of H. Here, the experimental form of $T_1^*(H)$ at the range below about 40 kOe is given by

$$[T_1^*(H)]^{-1} = C^* H^\alpha , \qquad (30)$$

where α and C^* are fitting parameters. They are tabulated in Table I. To the best of our knowledge, Eq. (30) is the first empirical form of $T_1^*(H)$ determined at a magnetic field range below about 40 kOe.

Now, by combining Eqs. (10) and (30), we propose a new composed form of $T_1^*(H)$ that is valid over the whole range of the magnetic field. It is shown as

$$[T_1^*(H)]^{-1} = C^* H^\alpha + (A^* H^3 + B^* H^5)$$
$$\times \coth(g^* \mu_B H / 2kT) . \qquad (31)$$

FIG. 4. $\Delta_\pi(\omega)$ for the F center in KBr is plotted as a function of pumping photon energies, E_{ph}, at $H = 18$ kOe and 2 K. Open circles are experimental points. The solid and dotted-dashed lines are theoretical plots of Eq. (28) with $\varepsilon_I = 0.020$ and 0, respectively. Dotted line is the F absorption band.

TABLE II. Fitting parameters T_1^{*-1} and ε_I with Eq. (28) to experimental data which are shown in open circles in Figs. 4 and 5.

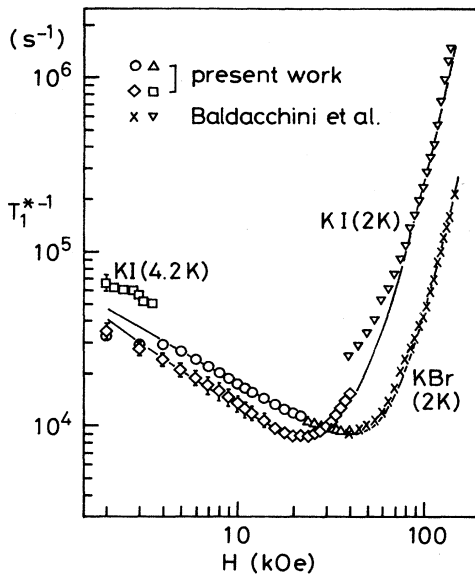|	H (kOe)	T (K)	τ_r^a (μs)	T_1^{*-1} (10^4 s^{-1})	ε_I
KBr	18	2	1.85	1.25	0.020
KI	3	4.2	2.5	5.6	0.016

^{a}Taken from Ref. 18.

FIG. 6. Inverse of the spin-lattice relaxation time in the RES, $[T_1^*(H)]^{-1}$ in Eq. (31), of F centers in KBr and KI is plotted with solid lines as a function of magnetic field at 2 K. The several symbols represent experimentally obtained points (see the text): the best-fit parameters are summarized in Table I together with data in Ref. 12.

In Fig. 6, the experimental data of $T_1^*(H)$ obtained at a higher-magnetic-field range by Baldacchini et al.[12] are shown by crosses for KBr and inverted open triangles for KI. The solid lines in Fig. 6 are the best-fit curves of Eq. (31). The fitting parameters of A^*, B^*, C^*, and α are listed in Table I, in which the values of A^* and B^* obtained in Refs. 11 and 12 are also listed. Baldacchini et al.[12] pointed out that the second term in Eq. (31) is due to the phonon modulation of hyperfine interaction between the F electron and surrounding nuclei,[2,12] and the third term is due to the orbital-lattice interaction,[2,12] respectively. Reflecting the fact that the value of T_1^* of the RES is several orders of magnitude smaller than T_1 of the GS, both A^* and B^* are likewise larger than A and B values of the GS reported in Ref. 12. Ham suggested that the larger values of A^* and B^* are caused by the dynamical vibronic effect in the Jahn-Teller system.[24]

Finally, theoretical curves of Eq. (28) are plotted with dotted lines in Figs. 2 and 3 for KBr and KI, respectively, by using appropriate parameter values of ε_l, ε_t, $P^*(\omega = 0$, $t = 0)$,[14] and $T_1^*(H)$ determined above. The agreement of the theoretical plots and the experimental points including signatures is fairly close. This reveals that the anomalous effect of $\Delta_\pi(\omega)$ is completely interpreted in the present scheme in terms of Eq. (28) with the form of $T_1^*(H)$ in Eq. (31).

B. Analysis of MCD(ω)

In 1979, Baldacchini et al. measured the H dependence of $\mathscr{S}_{\text{MCD}}(\omega)$ under the MSP conditions over the magnetic

field range between 0 and 80 kOe when irradiated with a He-Ne laser.[12] The data for KBr and KI at 1.85 K are plotted in Figs. 7 and 8 with open circles. They analyzed the data using Eq. (4) according to their argument, and determined the experimental form of Eq. (10) for $T_1^*(H)$ in the higher-magnetic-field range above 40 kOe. However, they have not accomplished the analysis of the data taken at a lower-magnetic-field range below 40 kOe.[25]

In the present work, with Eq. (29) derived, we analyzed their data of $\mathscr{S}_{\text{MCD}}(\omega)$ over the whole magnetic field range. Here, $x\alpha_0$ was taken as order unity. Theoretical curves of Eq. (29) for $\mathscr{S}_{\text{MCD}}(\omega)$ are plotted with solid lines in Figs. 7 and 8 as a function of H by adopting several known parameter values of P_s,[3] H_d,[20,21] $T_1^*(H)$, and our observed plot of $\Delta_\pi(\omega)$. These values adopted are tabulated in Table III. The agreement between the theoretical and experimental curves is satisfactory. From both figures, it is shown that the contribution of $\Delta_\pi(\omega)$ is not sizable in the range of H below 40 kOe. This means that $\mathscr{S}_{\text{MCD}}(\omega)$ is partly free from the imbalance of circular polarization for pumping.

It is astonishing to see that both $\mathscr{S}_{\text{MCD}}(\omega)$ and $\Delta_\pi(\omega)$, which have been observed in different countries with different apparatus, are described in terms of a common and equivalent form of $T_1^*(H)$ in Eq. (31). In particular, for KBr, both values of α and C^* in Table III are the same as those given in Table I. This means that the F concentration in KBr adopted in both schools happened to be almost the same amount. As for KI, the values of C^* in both tables coincides with each other, while the value of α in Table III is a little larger than that in Table I. This may occur if the F concentration in our school is slightly larger than that in the Italian school. In order to
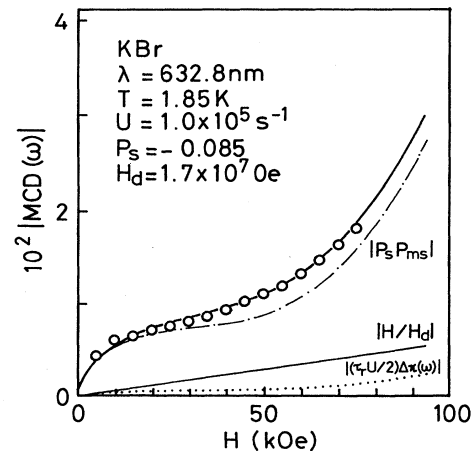

FIG. 7. The magnetic circular dichroism of F absorption under the MSP conditions for KBr is plotted as a function of magnetic field. Open circles are the experimental data by Baldacchini et al. in Ref. 12. The thick solid line is the theoretical plot of Eq. (29), when $x\alpha_0 = 1$. Its three components are plotted with a dotted-dashed line for $|P_s P_{ms}|$, a thin solid line for H/H_d, and a dotted line for $|(\tau_r U/2)\Delta_\pi(\omega)|$, respectively. The important parameters are listed in the figure.
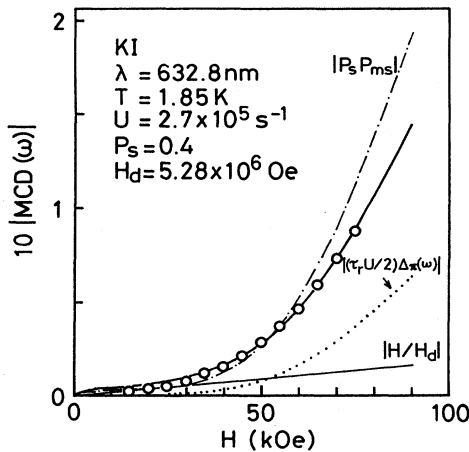
FIG. 8. The magnetic circular dichroism of F absorption under the MSP conditions for KI is plotted as a function of magnetic field. Open circles are the experimental data by Baldacchini et al. in Ref. 12. The thick solid line is the theoretical plot of Eq. (29), when $x\alpha_0 = 1$. Its three components are plotted with a dotted-dashed line for $|P_s P_{ms}|$, a thin solid line for H/H_d, and a dotted line for $|(\tau_r U/2)\Delta_\pi(\omega)|$, respectively. The important parameters are listed in the figure.

check this possibility, simultaneous measurement of $\mathcal{S}_{MCD}(\omega)$ and $\Delta_\pi(\omega)$ using the same specimen is scheduled.

C. Mechanism of $T_1^*(H)$ in lower-magnetic-field range

Because of the lack of a theoretical form to reproduce exactly the empirical form of Eq. (30), it would be hard to describe its mechanism of $T_1^*(H)$. However, we may point out that its characteristics below about 40 kOe in Fig. 6 are very similar to the experimental curve of $T_1(H)$ for GS, which had been measured for the densely colored KCl by Feldman et al.[26,27] They proposed that it was caused by the exchange interaction between two neighboring F centers in the GS.

On the basis of the idea of Feldman et al.,[26,27] Glinchuk, Grachev, and Deigen[28] derived a theoretical form of $T_1(H)$ for the spin-split sublevels in the GS [Eq. (32) in Ref. 28]. Although the form they derived is not the same as Eq. (31), we have found a close curve fitting of our data

in Fig. 6 with their theoretical form by choosing two parameters of γ and j^2, where γ is a factor proportional to a fraction of exchange pairs to total F concentration, and $j = J_0/g^*\mu_B$, where J_0 is an exchange coupling constant. The γ and the exchange angular frequency $\omega_0 = J_0/\hbar$ are 1.54 and 1.86×10^{11} s^{-1} for KBr, and 2.0 and 1.05×10^{11} s^{-1} for KI, where $g^* = 1.873$ and 1.686 for KBr and KI,[31] respectively. Showerer and Wolf had estimated ω_0 for the exchange pair of F centers in the GS for KCl.[29] We calculated $\omega_0 = 7.80 \times 10^5$ s^{-1} from their scheme and the value of j^2 for an F-center concentration $N_F = 3 \times 10^{16}$ cm^{-3} in Ref. 28. However, it would be hard to draw physically important quantities from the comparison of two ω_0 without knowledge of the exact wave functions in the RES. We have yet to point out a possible mechanism to account for $[T_1^*(H)]^{-1}$, that is, the exchange effect.

Furthermore, from Eq. (30), we may predict that $[T_1^*(H)]^{-1}$ shows minimum value at a specific magnetic field, H_s: this is shown in Fig. 6. Nearly the same characteristics were observed in the H dependence of T_1 for the GS $[T_1(H)]^{-1}$, as shown in Ref. 3. We point out, particularly, that H_s in $[T_1(H)]^{-1}$ for $N_F = 3 \times 10^{18}$ cm^{-3} is nearly equal to that of $[T_1^*(H)]^{-1}$ for $N_F = 3 \times 10^{16}$ cm^{-3}. This implies that hundreds of times-larger concentrations of F centers in the GS should be necessary to exert the same amount of exchange effect as that in the RES. This implication shows qualitatively that the orbital wave function of the RES is spread more than that of F centers in the GS. However, again we are faced with the same difficulty as mentioned in the preceding paragraph. Namely, no further argument could be progressed without knowing the physical meaning of the parameters of α and C^* as well as these values for the GS. A detailed analysis of the exchange effect is left as a future problem.

D. Optical detection of ESR of F centers

So far, the optical detection of ESR (ODESR) for GS and RES of the F centers had been successfully performed by two different ways. The first was to detect the induced change of the MCD caused by the resonant microwave for the electron-spin systems.[3,30,31] The second was to monitor the change of the luminescence intensity of the F center caused by the resonant microwave transition.[32,33] The method was based on the Porret and Lüty

TABLE III. Fitting parameters of Eq. (29) to the H dependence of $\mathcal{S}_{MCD}(\omega)$ observed in Ref. 12. The fitting parameter values of T_1^{*-1} in Eq. (31) are also listed.

	P_s[a]	H_d[b] (10^6 Oe)	U[c] (10^5 s^{-1})	A^* (10^{-11} Oe^{-3}s^{-1})	T_1^{*-1} B^* (10^{-21} Oe^{-5}s^{-1})	C^* (10^7 Oe$^{-\alpha}$s^{-1})	α
KBr	-0.085	17.0	1.0	1.5	2.6	0.50	-0.613
KI	0.40	5.28	2.7	5.7	3.0	1.13	-0.85

[a]Taken from Ref. 3.
[b]Taken from Ref. 21.
[c]Estimated approximately.

effect.[34]

In our laboratory, we proposed an entirely different method from the above two methods. The working principle is to monitor the induced change of the MCP of the F-center emission caused by the ESR transition in the Kramers doublet of either GS or RES. This idea was first tested for the paramagnetic component of the MCP observed under the SSP conditions.[35,36]

In this subsection, we describe a method of measuring the ODESR by controlling the changes in the NESP term in $\Delta_\eta(\omega)$ with resonant microwaves. One of the typical ODESR traces observed for KBr is shown in Fig. 9, when sending microwaves at 50 GHz: The two dips found in $\Delta_\eta(\omega)$ at about 20-kOe range are the ODESR signals of GS and RES, respectively, counting from low to high magnetic fields. The order estimate of $\Delta_\eta(\omega)$ from the contribution to the ODESR in the first term in Eq. (27) shows a negligibly small contribution in comparison with that of the second term. This clearly shows that *the induced change of the NESP in the MSP conditions mostly dominates the signal of the ODESR*. The values of the g factor and half-width of the RES and GS determined for KBr, KI, and RbCl are listed in Table IV. These values almost agree with those determined already by other authors using different methods:[3,32,35,36] they are also summarized in Table IV. This agreement shows that the values determined by our method would be reasonable and convincing in comparison with the other two methods.

A theoretical form of the ODESR signal intensity, $\delta(\Delta_\eta(\omega; W \text{ or } W^*))$ for the GS or RES, can be deduced as the difference between $\Delta_\eta(\omega; W$ or $W^*)$ and $\Delta_\eta(\omega; W = W^* = 0)$, where W and W^* are the ESR tran-

sition probabilities between Kramers sublevels in the GS and RES, respectively. Here, the $\Delta_\eta(\omega; W$ or $W^*)$ is derived by solving the rate equations (14), in which the ESR transition terms including W or W^* are added in. As was argued in the preceding paragraph, only the $\Delta_\pi(\omega; W$ or $W^*)$ term is necessary for estimating the intensity of the ODESR. After a tedious calculation using the additional assumptions that $(W$ and $W^*) < U < \tau_r^{-1}$, $1 \gg 2\varepsilon_t L$, and $\Delta_\pi(\omega; 0) \gg \varepsilon_I P_s^2$, the approximate forms of the ODESR intensities for the RES and GS are shown as follows:[23]

$$\delta(\Delta_\eta(\omega; W^*))$$
$$\simeq -[W_r/(1+L+W_r)]\Delta_\pi(\omega; W=W^*=0) , \quad (32a)$$

and

$$\delta(\Delta_\eta(\omega; W))$$
$$\simeq -2[W_g/(1+L+2W_g)]\Delta_\pi(\omega; W=W^*=0) , \quad (32b)$$

where $W_r = \tau_r W^*/\varepsilon_t$ and $W_g = W/\varepsilon_t U$, respectively. Equations (32) are calculated solely for the homogeneously broadened line.

The peak intensity of the ODESR signal for the GS and RES is plotted in Fig. 10 as a function of laser power, and in Fig. 11 as a function of microwave power. Both characteristics show quite the same tendency as those observed under the SSP conditions.[36] Figure 10 shows that the ODESR intensity of the RES is nearly independent of U. This fact is endorsed by Eq. (32a), which is clearly independent of U. This is caused by the fact that the NESP in the RES is independent of U under the MSP conditions. The solid lines in Fig. 10 are theoretical plots of Eqs. (32a) and (32b). Furthermore, the characteristics in Fig. 11 are also explained by adopting Eqs. (32). The
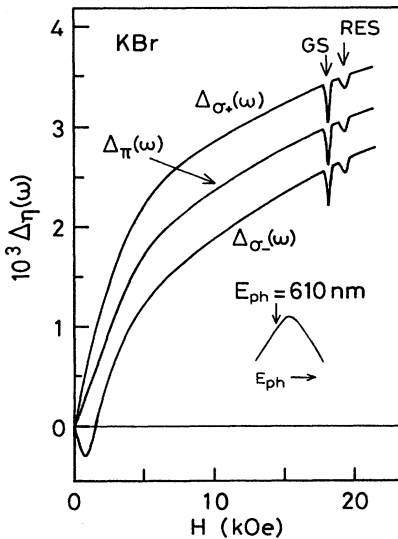

FIG. 9. The magnetic field dependences of $\Delta_\eta(\omega)$, where $\eta = \sigma_+, \sigma_-,$ and π, are plotted with solid lines for KBr, when pumped with wavelength of 610 nm at 2 K. Two dips observed in each line at around 18 kOe are ESR lines corresponding to GS and RES with a microwave at 50 GHz.
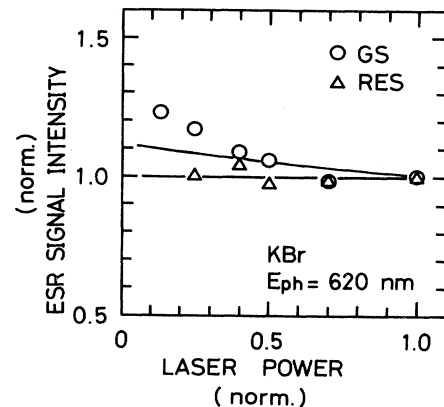

FIG. 10. ESR intensity of GS and RES in KBr at 2 K plotted as a function of pumping laser power at 620 nm, which is proportional to the net pumping rate U. Solid lines are theoretical plots of Eqs. (32) calculated for the homogeneously broadened line.

TABLE IV. Values of g factor and ODESR half-width for the relaxed excited state (RES) and ground state (GS) of F centers in KBr, KI, and RbCl. Results by other authors are summarized.

Crystal	RES g^*	Half-width (Oe)	GS g	Half-width (Oe)	References
KBr	1.868	223	1.984	125	This work and 36
	1.862	270	1.982	146	3
	1.873	234	1.984	147	31
	1.873	256	1.984	147	32
	1.87	260	1.98	150	35
KI	1.687	588	1.964	258	This work and 36
	1.627	575	1.964	263	3
	1.686	541	1.964	265	31
	1.630	570	1.964	265	32
RbCl	1.937	178	1.980	499	This work and 36
	1.930	188	1.980	522	31
	1.85	300	1.98	430	35

solid lines in the figure are theoretical plots of Eqs. (32).

Finally, it should be worth noticing that the sensitivity of the present method is approximately more than ten times as large as that of the SSP conditions, possibly because of the adoption of the modulation method for optical measurement [see Eq. (27)]. For example, the ODESR can be observed in the MSP conditions even in the range where E_{ph} is larger than E_0. On the contrary, under the SSP conditions, no ODESR was observed in this range. Therefore, we recommend the application of this method widely for the ODESR of the defects in solids.
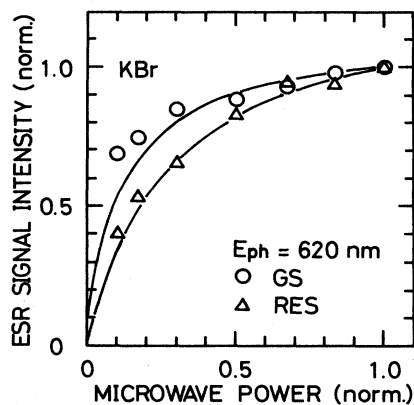

FIG. 11. ESR intensity of GS and RES in KBr at 2 K plotted as a function of microwave power applied, when pumped with wavelength of 620-nm laser light. Solid lines are theoretical plots of Eqs. (32) calculated for the homogeneously broadened line.

V. CONCLUSION

We have studied dynamical magneto-optical effects of the F center observed under the modulated- and saturated-pumping (MSP) conditions, when the circular polarization of intense pumping laser light is periodically alternated between right and left (σ_+ and σ_-) with angular frequency ω. Under the MSP conditions, we propose that the nonequilibrium spin polarization (NESP), which could be built up in the relaxed excited state (RES), P_{ms} in Eq. (18), can vary sinusoidally with ω in an optical-pumping cycle (OPC). This proposal is formulated in the first-order approximation to the rate equations governing the OPC, in which the imbalance parameter of σ_+ and σ_- components of pumping light intensity is included. This oscillating NESP gives rise to the magnetic circular dichroism [$\mathcal{S}_{MCD}(\omega)$] in the absorption and the magnetic circular polarization [$\Delta_\eta(\omega)$] in the emission, where η represents the polarization of the analyzer (σ_+, σ_-, and linear π) through which the η components of polarization of $\Delta_\eta(\omega)$ are detected distinctly. These quantities have been observed through a lock-in amplifier operated at ω.

Based on the theoretical scheme mentioned above, we have derived the theoretical expressions for the analysis of $\mathcal{S}_{MCD}(\omega)$ and $\Delta_\eta(\omega)$ which are observed in the MSP conditions. The result is that the $\Delta_\pi(\omega)$ in Eq. (1), which had been called the anomalous effect, is a net emission intensity sinusoidally oscillating with ω, while the electron is performing the OPC with a pumping rate U. We have shown that both $\mathcal{S}_{MCD}(\omega)$ and $\Delta_\eta(\omega)$ are commonly represented in terms of the spin-lattice relaxation time T_1^* in the Kramers sublevels in the RES.

We have measured $\Delta_\eta(\omega)$ of F centers in KBr and KI at 2 K as a function of magnetic field H up to 40 kOe, as well as of the pumping photon energy E_{ph}. These experimental data observed and the H dependence of $\mathcal{S}_{MCD}(\omega)$, which had been measured by Baldacchini et al.,[12] are an-

alyzed using the present theoretical expressions in Eqs. (27) and (29). The curve fitting was performed by adopting fitting parameters of ε_I and an empirical form of the H dependence of $T_1^*, T_1^*(H)$. $[T_1^*(H)]^{-1}$ is represented as being proportional to H^α below 40 kOe, where α is a negative constant. We propose that the $T_1^*(H)$ is caused by the exchange interaction between neighboring F centers in the RES. With this information, the anomalous effect of the $\Delta_\pi(\omega)$ is fully understood.

Finally, we have tested the optical detection of the electron-spin resonance (ODESR) of GS and RES for KBr, KI, and RbCl at 2 K by monitoring the change in $\Delta_\eta(\omega)$ that is induced by the resonant microwave transitions at 50 GHz. The ODESR signals observed are in-dependent of η, and is principally dependent on the NESP. The ODESR signal intensity and its sign for both GS and RES depend on the laser power as well as microwave power. The dependences are explained semi-quantitatively by using forms derived on the basis of the present scheme.

ACKNOWLEDGMENTS

APPENDIX: STRICT SOLUTION OF EQS. (17)

The exact forms of four terms in Eqs. (17), when $\varepsilon_I = 0$, have been solved in Ref. 14. They are shown as follows. P_m is the same form as P in Eq. (5),

$$|P_m(\omega)| = \{(\varepsilon_t U/\tau_r)^2[(1+L)P_s + P^*(0)]^2 + (U/2)^2 P_s^2 \omega^2\}^{1/2}/[A(\omega)]^{1/2}, \tag{A1}$$

$$P_m^* = P_m + 2\varepsilon_t[\langle P^*\rangle - (1+L)\langle P\rangle]/[(1+T_1/T_p)(1+2\varepsilon_t L)], \tag{A2}$$

and

$$|P_m^*(\omega)| = (1-2\varepsilon_{rl})(1/\tau_r)\{[(\delta\varepsilon U/2 + \kappa/T_1)^2 + \kappa^2\omega^2]\}^{1/2}/[A(\omega)]^{1/2}, \tag{A3}$$

with

$$A(\omega) = (U/2 + 1/\tau_r + 1/T_1 + 1/T_1^*)^2\omega^2 + \{(\varepsilon_t U/\tau_r)[1+L+(T_1/T_p)(1+2\varepsilon_t L)] - \omega^2\}^2. \tag{A4}$$

P_m and P_m^* are the NESP in the GS and RES. Their approximate forms are derived under the MSP conditions in the ω range covering $\varepsilon_t U < \omega < \tau_r^{-1}$. We denote their approximate forms as P_{ms} and P_{ms}^*. P_{ms}^* is found to be approximately equal to P_{ms}. The characteristic relation is shown in Eq. (18).

These equations can be reduced to the equations that have been previously derived by several authors. For instance, under the limiting conditions when $\varepsilon_{rl} = 0$, $\varepsilon_t = \varepsilon_0$, $T_1 \to \infty$, $T_1^* \to \infty$, $U \ll \tau_r^{-1}$, and using relations $(\varepsilon_0 U - \tau_r \omega^2)^2 \simeq \varepsilon_0^2 U^2 + \tau_r^2 \omega^4$, $P(\omega; \delta\varepsilon = 0, P_s \neq 0)$, and $P^*(\omega; \delta\varepsilon = 0, P_s \neq 0)$, Eqs. (A1) and (A3) are reduced to $P(1)$ [Eq. (10a) in Ref. 13] and $P_p(1)$ [Eq. (11a) in Ref. 13], respectively. Moreover, $P(\omega; \delta\varepsilon \neq 0, P_s = 0)$ and $P^*(\omega; \delta\varepsilon \neq 0, P_s = 0)$ are reduced to $P(2)$ [Eq. (10b) in Ref. 13] and $P_p(2)$ [Eq. (11b) in Ref. 13], respectively.

On the other hand, if adopting $\varepsilon_{rl} = 0$ and $\varepsilon_0 = \varepsilon_t = \varepsilon$, when $P_s \neq 0$, $\delta\varepsilon = 0$, and $L_0 = \tau_r/(2\varepsilon_0 T_1^*)$, together with $T_p^0 = (\varepsilon U)^{-1}$, Eq. (17a), which consists of sum of Eqs. (5) and (A1), is derived as follows.
$P_0(\omega = 0, t = 0; \delta\varepsilon = 0, P_s \neq 0)$

$$= [(1+L_0)P_s + L_0\langle P^*\rangle + (T_p^0/T_1)(1+2\varepsilon_0 L_0)\langle P\rangle]/[1+L_0+(T_p^0/T_1)(1+2\varepsilon_0 L_0)+L_0 P_s\langle P^*\rangle]. \tag{A5}$$

Equation (A5) is equivalent to the polarization in the GS [Eq. (21) in Ref. 3]. Thus, Eq. (21) in Ref. 3 should be read as Eq. (A5).

[1]N. V. Karlov, J. Margerie, and Y. Merle-D'Aubigné, J. Phys. (Paris) 24, 717 (1963).
[2]H. Panepucci and L. F. Mollenauer, Phys. Rev. 178, 589 (1969).
[3]L. F. Mollenauer and S. Pan, Phys. Rev. B 6, 772 (1972).
[4]A. Winnacker, K. E. Mauser, and B. Niesert, Z. Phys. B 26, 97 (1977).
[5]K. E. Mauser, B. Niesert, and A. Winnacker, Z. Phys. B 26,

107 (1977).

[6]M. P. Fontana and D. B. Fitchen, Phys. Rev. Lett. **23**, 1497 (1969).

[7]G. Baldacchini, U. M. Grassano, and A. Tanga, Phys. Rev. B **16**, 5570 (1977).

[8]K. Imanaka, T. Iida, and H. Ohkura, J. Phys. Soc. Jpn. **44**, 1632 (1978).

[9]K. Imanaka, T. Wada, T. Iida, and H. Ohkura, Solid State Commun. **27**, 1009 (1978).

[10]H. Ohkura, K. Iwahana, M. Tanaka, K. Tara, and K. Imanaka, J. Phys. Soc. Jpn. **49**, 2296 (1980).

[11]G. Baldacchini and U. M. Grassano, Phys. Rev. B **28**, 4855 (1983).

[12]G. Baldacchini, U. M. Grassano, and A. Tanga, Phys. Rev. B **19**, 1283 (1979).

[13]G. Baldacchini, A. Tanga, and U. M. Grassano, Phys. Rev. B **20**, 4357 (1979).

[14]H. Ohkura, K. Tara, N. Akiyama, K. Iwahana, and Y. Mori, J. Phys. Soc. Jpn. **51**, 3615 (1982).

[15]N. Akiyama, K. Kawano, Y. Mori, and H. Ohkura, J. Phys. Soc. Jpn. **53**, 1927 (1984).

[16]H. Ohkura, Cryst. Latt. Def. Amorph. Mat. **12**, 401 (1985).

[17]Y. Mori, H. Hanzawa, and H. Ohkura, J. Lumin. **38**, 159 (1987).

[18]R. K. Swank and F. C. Brown, Phys. Rev. Lett. **8**, 10 (1962); Phys. Rev. **130**, 34 (1963).

[19]S. Muramastu, N. Akiyama, Y. Mori, and H. Ohkura, J. Phys. Soc. Jpn. **55**, 2811 (1986).

[20]C. H. Henry and C. P. Slichter, in *Physics of Color Centers*, edited by W. B. Fowler (Academic, New York, 1968), Chap. 6.

[21]J. Mort, F. Lüty, and F. C. Brown, Phys. Rev. **137**, A566 (1965).

[22]Notice that Eq. (9) is solely valid when the *F* center is pumped with linearly polarized light (π polarization). In the π pumping, however, P_s in Eq. (3) vanishes automatically. Thus, the $\mathscr{S}_{\text{MCD}}(\omega)$ in Eq. (4) is presented only by the first term that is a diamagnetic part. So that, it would be unreasonable to derive Eq. (10) by simply inserting Eq. (9) into Eq. (4).

[23]N. Akiyama, Ph.D. thesis, Osaka City University, 1985 (in Japanese).

[24]F. S. Ham, in *Electron Paramagnetic Resonance*, edited by S. Geschwind (Plenum, New York, 1972), Chap. 1.

[25]Their analysis of $\mathscr{S}_{\text{MCD}}(\omega)$ for KBr at a lower-magnetic-field range is quite different from our present analysis. In fact, they assumed that the H dependence of $\mathscr{S}_{\text{MCD}}(\omega)$ could be separated into two parts: one is the diamagnetic part and the other is the paramagnetic contributions of unknown origin, which show a saturated behavior at about 15 kOe.

[26]D. W. Feldman, R. W. Warren, and J. G. Castle, Jr., Phys. Rev. **135**, A470 (1964).

[27]R. W. Warren, D. W. Feldman, and J. G. Castle, Jr., Phys. Rev. **137**, A1347 (1964).

[28]M. D. Glinchuk, V. G. Grachev, and M. F. Deigen, Fiz. Tverd. Tela (Leningrad) **8**, 3354 (1967) [Sov. Phys.—Solid State **8**, 2678 (1967)].

[29]M. Schwoerer and H. C. Wolf, Z. Phys. **175**, 457 (1963).

[30]L. F. Mollenauer, S. Pan, and S. Yngvesson, Phys. Rev. Lett. **23**, 689 (1969).

[31]H. J. Reyher, K. Hahn, Th. Vetter, and A. Winnacker, Z. Phys. B **33**, 357 (1979).

[32]Y. Ruedin, P. A. Schnegg, C. Jaccard, and M. Aegerter, Phys. Status Solidi B **54**, 565 (1972).

[33]K. Murayama, K. Morigaki, and H. Kanzaki, J. Phys. Soc. Jpn. **38**, 1623 (1975).

[34]F. Porret and F. Lüty, Phys. Rev. Lett. **26**, 843 (1971).

[35]K. Imanaka, T. Wada, M. Tanaka, and H. Ohkura, J. Phys. Soc. Jpn. **45**, 2041 (1978).

[36]N. Akiyama, Y. Mori, and H. Ohkura, Radiat. Eff. **72**, 277 (1983).